OPEN

Citation: Cell Death and Disease (2013) 4, e783; doi:10.1038/cddis.2013.314

www.nature.com/cddis

Cuprous oxide nanoparticles inhibit the growth and metastasis of melanoma by targeting mitochondria

Y Wang[1,2,3], F Yang[4], H-X Zhang[1,2], X-Y Zi[1,2], X-H Pan[5], F Chen[1,2], W-D Luo[3], J-X Li[1,2], H-Y Zhu*[,1,2] and Y-P Hu*[,1,2]

Metal and its oxide nanoparticles show ideal pharmacological activity, especially in anti-tumor therapy. Our previous study demonstrated that cuprous oxide nanoparticles (CONPs) selectively induce apoptosis of tumor cells *in vitro*. To explore the anti-tumor properties of CONPs *in vivo*, we used the particles to treat mouse subcutaneous melanoma and metastatic lung tumors, based on B16-F10 mouse melanoma cells, by intratumoral and systemic injections, respectively. The results showed that CONPs significantly reduced the growth of melanoma, inhibited the metastasis of B16-F10 cells and increased the survival rate of tumor-bearing mice. Importantly, the results also indicated that CONPs were rapidly cleared from the organs and that these particles exhibited little systemic toxicity. Furthermore, we observed that CONPs targeted the mitochondria, which resulted in the release of cytochrome C from the mitochondria and the activation of caspase-3 and caspase-9 after the CONPs entered the cells. In conclusion, CONPs can induce the apoptosis of cancer cells through a mitochondrion-mediated apoptosis pathway, which raises the possibility that CONPs could be used to cure melanoma and other cancers.
Cell Death and Disease (2013) **4,** e783; doi:10.1038/cddis.2013.314; published online 29 August 2013
Subject Category: Cancer

In recent years, with the rapid development of nanoscience and nanotechnology, many nanomedicines, such as gold nanoparticles,[1,2] metallic multi-segments,[3] silicon nanowire,[4,5] iron core-gold shell nanoparticles,[6] chitosan nanoparticles,[7] and gold nanorods,[8] have been designed for tumor therapy. When the conventional therapies, including surgical interventions , radiation, and cytotoxic chemotherapies, are ineffective in curing cancer, it is necessary to explore novel drugs.[9,10] Nanomedicines have been emerging as one of these new treatment options.[11,12]

Arsenic trioxide, which represents one of the new types of medicines and is derived from a famous, traditional Chinese remedy, has been used to successfully treat acute promyelocytic leukemia.[13] Inspired by this research, we found azurite ore mentioned in *Shen Nong's Herbal*, a traditional Chinese medical text. This medicine was used and recorded as an anti-tumor medicine and is now known to be a type of copper compound. By combining nanomedicine with traditional Chinese medicine, we tried to examine the possibility of applying cuprous oxide nanoparticles (CONPs) to cancer therapy.

Melanoma is highly aggressive, leaving untreated patients with a median survival of <12 months.[14] In recent years, the incidence of melanoma has been increasing rapidly.[15] Melanoma is a cancer that is difficult to cure by conventional therapy, which is one of the reasons why we chose to focus on melanoma in this study.[16–18] The other reason is that our previous research has shown that CONPs can selectively induce apoptosis and inhibit the proliferation of tumor cells *in vitro* and that melanoma cells are highly sensitive to CONPs,[19] suggesting that CONPs may be used in the treatment of melanoma. To verify this hypothesis, we sought to test the anti-tumor capability of CONPs *in vivo*. We established two types of tumor-bearing mouse models based on B16-F10 melanoma cells, representing subcutaneous melanoma and metastatic lung tumors. Following an intratumoral injection of CONPs into the subcutaneous melanoma, we found that the growth of the tumors was significantly inhibited and that the survival rate of the mice was markedly increased. The results of the systemic therapy showed that CONPs not only repressed the metastasis and proliferation of B16-F10 cells but also were rapidly cleared from the organs, resulting in little hepatic and renal toxicities in mice.

Concerning the anti-tumor mechanism underlying inorganic nanomedicines, it has been reported that many of these nanomedicines with chemical modifications can kill tumor cells by targeting the nucleus[20] or other organelles[21–23] or by increasing the reactive oxygen species (ROS) level in tumor cells. In the current study, we found that CONPs without chemical modification targeted the mitochondria specifically, caused cytochrome C (Cyt C) release, and activated caspase-3 and caspase-9, which demonstrated that CONPs induced

[1]Department of Cell Biology, Second Military Medical University, Shanghai, P. R. of China; [2]Center for Stem Cell and Medicine, The Graduate School, Second Military Medical University, Shanghai, P. R. of China; [3]School of Clinical Medicine, Second Military Medical University, Shanghai, P. R. of China; [4]School of Pharmacy, Second Military Medical University, Shanghai, P. R. of China and [5]Department of Genetics, Yale University School of Medicine, New Haven, CT, USA
*Corresponding author: H-Y Zhu or Y-P Hu, Department of Cell Biology, Second Military Medical University, 800-Xiang Yin Road, Shanghai 200433, P. R. of China. Tel: +86 21 81870943; Fax: +86 21 81870948; E-mail: yphu@smmu.edu.cn or zinnia69@163.com
Keywords: cuprous oxide nanoparticles; melanoma; apoptosis; mitochondrion-mediated apoptosis; anti-tumor nanomedicine
Abbreviations: CONPs, cuprous oxide nanoparticles; ROS, reactive oxygen species; IC50, half-maximal inhibitory concentration; TEM, transmission electron microscopy; Cyt C, cytochrome C; Z-VAD-FMK, carbobenzoxy-valyl-alanyl-aspartyl-[O-methyl]-fluoromethylketone; DCF-DA, dihydrodichlorofluorescein diacetate; MTT, 3-(4,5-dimethylthiazol-2yl)- 2,5-diphenyl tetrazolium bromide; EMT, epithelial–mesenchymal transition
Received 18.5.13; revised 05.7.13; accepted 29.7.13; Edited by G Melino

the apoptosis of tumor cells by initiating a mitochondrion-mediated apoptosis signaling pathway. Our results strongly suggest that CONPs can ultimately be applied to the treatment of melanoma and other cancers as a new type of anti-tumor nanomedicine.

Results

CONPs induce apoptosis and inhibit migration of tumor cells *in vitro*. CONPs were synthesized and characterized as in our previous study,[19] and the diameter of the CONPs ranged from 40 to 110 nm. Cell viability following CONPs treatment was then evaluated using the 3-(4,5-dimethylthiazol-2 yl)-2,5-diphenyl tetrazolium bromide (MTT) assay. Our data showed that CONPs could kill B16-F10 and HeLa cells in a dose- and time-dependent manner. The half-maximal inhibitory concentration (IC50) for the B16-F10 cells was 1.992 μg/ml after 48 h of CONPs treatment, whereas for the HeLa cells, it was 8.28 μg/ml after 48 h (Supplementary Figures S1a and b). In our previous study, we found that the IC50 values for normal mouse embryonic fibroblast cells and 293 T cells were 27.00 and 14.22 μg/ml, respectively, indicating that CONPs are selectively cytotoxic to tumor cells.[19] In the current study, the B16-F10 cells were highly sensitive to CONPs, with an IC50 value that was one of the lowest among the cells we tested. In addition, Annexin V- and PI-based apoptosis and necrosis discrimination assays were performed on B16-F10 cells, which were exposed to CONPs for 24 h and 48 h. The result exhibited that CONPs significantly induced the apoptosis in B16-F10 cells in a dose- and time-dependent manner (Supplementary Figure S1c).

In the meantime, Transwell assays were performed to test whether migration and invasion of the tumor cells were inhibited by CONPs *in vitro*. As shown in Supplementary Figure S2, migration and invasion of B16-F10 cells were all inhibited significantly by CONPs at the concentration of 1.25 and 2.5 μg/ml ($^*P<0.05$, Student's *t*-test). Real-time RT-PCR results showed that CONPs might downregulate the expressions of epithelial–mesenchymal transition (EMT)-related genes, *N-cadherin* (mesenchymal marker, *Cdh2*), *Twist1*, and *Snail1* ($^*P<0.05$, Supplementary Figure S3). However, it may have no effects on *E-cadherin* (epithelial marker, *Cdh1*) expression.

CONPs inhibit the growth and metastasis of melanoma in tumor-bearing mice. To establish a subcutaneous melanoma model, B16-F10 cells in the exponential growth phase were transplanted subcutaneously behind the inguen of C57BL/6 mice. CONPs were dissolved in a 5% glucose solution using an ultrasonic mixer. When the tumors had grown to an approximate diameter of 5–7 mm, the CONPs solution or a 5% glucose solution without CONPs (control) were injected into the tumors (the time point was marked as day 0). In the CONP treatment group, CONPs were injected at 16 mg/kg (approximately 400 μg CONPs) once per day, from day 0 to day 16. We found that, at each test time point, the diameters of all the tumors in the CONP group were visibly smaller than the tumors of the glucose group (Figures 1a and b). Additionally, the tumor masses of the CONP group were significantly lower than the masses recorded for the glucose group (Figure 1c). These results showed that the tumor growth was markedly inhibited by CONPs *in vivo*. Consistent with this finding, CONPs also improved the survival rate and lengthened the lifetime of the melanoma-bearing mice compared with the mice in the glucose group (Figure 1d). A TUNEL assay was used to confirm that CONPs can induce the apoptosis of B16-F10 cells *in vivo* (Figures 1e, f (as a control) and g, $^*P<0.05$, Student's *t*-test), which results in the suppression of tumor growth.

The results of the systemic therapy in mice bearing B16-F10 cell-based metastatic lung tumors were positive. CONPs were injected into tumor-bearing mice through the vena orbitalis posterior once per day. Fifteen days later, the lungs of the mice were collected. Our data showed that the number of tumor nodules on the lung surfaces of the mice in the CONP group was significantly lower than the number of nodules in the lungs of mice in the glucose group (Figures 1h and i, $^*P<0.05$, Student's *t*-test).

CONPs were rapidly cleared by the mice. To examine the *in vivo* safety and toxicity of CONPs, we injected C57BL/6 mice with an intravenous dose of CONPs (total CONP administration of 6 mg/kg). The toxicity was monitored in the next 7 days. No mice died, and all the mice lived normally over the next 7 days, at which time point the serum and certain organs of the mice in the CONPs and glucose groups were collected. The results of the serum test showed that the alanine aminotransferase, glutamic-oxaloacetic transaminase, albumin, and blood urea nitrogen were at normal levels in the CONP group (Figure 2a), because there were no statistically significant differences between the CONPs and glucose groups, suggesting no hepatoxicity or renal toxicity if any. Consistent with this result, the lung, kidney, liver, and spleen presented virtually no obvious histological changes in the HE-stained images (Figure 2b, Supplementary Figure S4a as control from the health mice), indicating that there were little toxic effect due to the administration of CONPs in mice.

In the clearance assay, an atomic absorption spectrometer was used to test the concentration of copper in the mouse spleen, lung, liver, and kidney at 4 h and 7 days after injection. The results showed that the concentration of copper in the tested organs decreased to a level equal to the copper level in the control group by 7 days after the injection, which suggested that CONPs were rapidly cleared by the mice (Figure 2c). In addition, the weights of the tumor-bearing mice in the CONP group were constant, whereas the weights of the glucose group decreased dramatically during the 15 days of systemic therapy in the metastatic lung tumor model (Figure 2d, $^*P<0.05$, Student's paired *t*-test). Hepatoxicity and renal toxicity were not observed in this experiment of the CONPs (Figure 2e). Furthermore, HE-stained images of the mouse major organs showed that there were no significant histological changes (Supplementary Figure S4b).

CONPs target mitochondria in cells and induce apoptosis by a mitochondrion-mediated apoptosis pathway. From TEM (transmission electron microscopy) images, we can discover that CONPs entered mitochondria in the B16-F10 cells by transporting or by uptaking (Figures 3a–d).

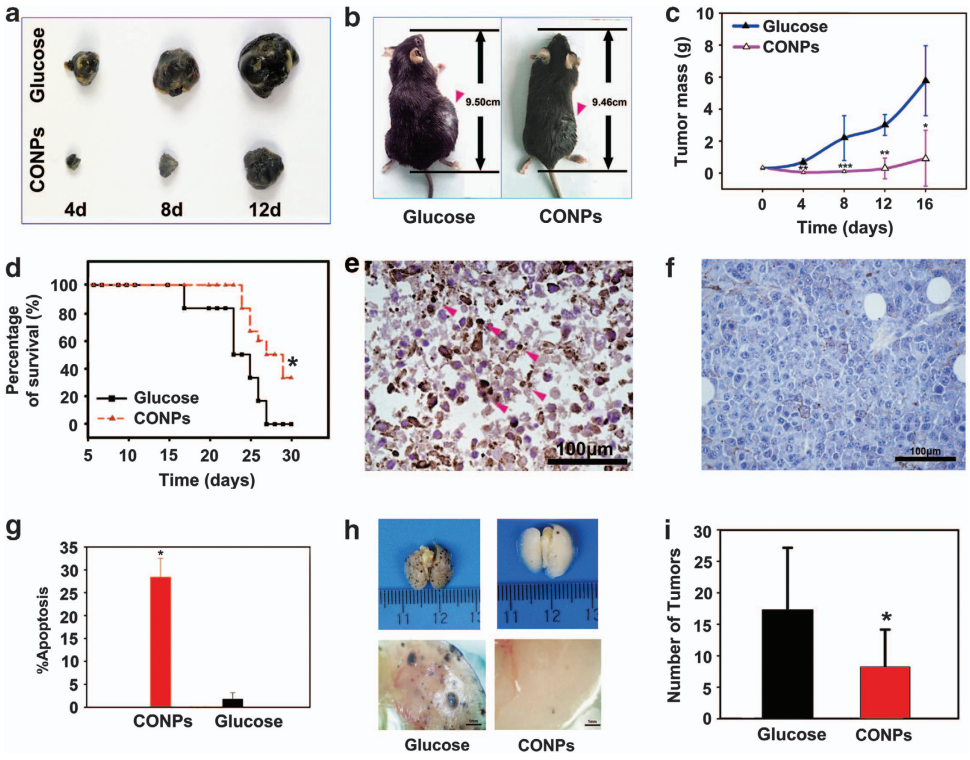

Figure 1 Anti-tumor effects of CONP therapy on subcutaneous melanoma and metastatic lung tumors. (**a**) Representative images of stripped subcutaneous tumors. The diameters of the subcutaneous tumors of the CONP group were obviously smaller than the diameters observed in the glucose group. (**b**) Representative images of mice bearing subcutaneous melanoma from the same study at day 12. The tumors of the CONP group were significantly smaller than the tumors of the glucose group. (**c**) Plot of tumor mass *versus* time. Day 0 was the starting of the treatment. The mice bearing subcutaneous tumors were euthanized when exhibiting signs of illness or death. The tumor masses of the deceased mice were not included after the day of death. Each group initially contained six mice. The error bars represent ± S.D. The tumors of the CONP group were significantly smaller when compared with the tumors of the control mice (*$P<0.05$, for day 16; **$P<0.005$, for days 4 and 12; and ***$P<0.001$, for day 8; Student's paired *t*-test, $n=6$). (**d**) Survival plot of mice bearing subcutaneous tumors. The survival of mice treated with CONPs was significantly longer than the mice in the glucose group (*$P<0.05$, log-rank test, $n=6$). Day 5 was the first day of CONPs injection. (**e**) TUNEL (terminal deoxinucleotidyl transferase-mediated dUTP-fluorescein nick end labeling)-stained assay of the subcutaneous tumors of CONP-treated mice on day 8. The image shows that CONPs induced the apoptosis of the tumor cells *in vivo* (as indicated by pink arrow). (**f**) TUNEL-stained assay of the control mice in the glucose group. (**g**) Statistical analysis of the positive cells in the TUNEL assay showed that the CONPs induced apoptosis of the tumor cells *in vivo* (*$P<0.05$, Student's *t*-test). (**h**) Representative lung images from mice in the metastatic lung tumor experiment. The average diameter of the lung tumors of the CONP group was significantly lower than the diameter of the tumors of the glucose group. (**i**) Number of tumors, counted using an anatomical lens, in the lungs of mice 15 days after the initiation of treatment. Regions of lung metastasis, which were >0.1 mm in diameter, were recorded. Treatment with CONPs significantly reduced the number of metastases (*$P<0.05$, Student's paired *t*-test, $n=6$)

At the same time, many cells with typical apoptotic phenotype were also found (Figures 3e and f). Both JC-1-stained images and the flow cytometry assay results indicated that the mitochondrial membrane potential dropped significantly and in a dose-dependent fashion in B16-F10 and HeLa cells treated with CONPs (Figures 4a and b). Supplementary Figure S5a summarizes our finding that the fluorescence intensity ratio of red to green decreased dramatically and in a dose-dependent manner. Additionally, western blotting revealed an increased amount of Cyt C in the cytoplasm (Figure 4c), which is deemed to be one of the most important factors in the apoptosis pathway. A significant increase in caspase-3 and caspase-9 activity (Figure 4d and Supplementary Figure S5b) were observed at certain time points in the cells treated with CONPs by western blot and activity assay. When using Z-VAD to block the caspases activity, we found that the Z-VAD increased the cell viability at the same dose of CONPs compared with the Z-VAD-negative group (Supplementary Figure S5c, *$P<0.05$, Student's *t*-test). Furthermore, we also found that the activation of caspase-3 was upregulated in the subcutaneous melanoma being treated with CONPs for 12 days (Supplementary Figure S5d, *$P<0.05$, Student's *t*-test). Finally, intracellular ROS levels in both HeLa and B16-F10 cells increased significantly after treatment with CONPs (Figure 4e), which is a sign of mitochondrial damage.

Discussion

We report here a comprehensive description on the anti-tumor capacity of CONPs *in vivo*. As a member of nanomaterials, CONPs in our research are a type of inorganic nanomaterial without any chemical modification, which have different characteristics from the other nanoparticles with anti-tumor activities. The recent studies by others have shown that gold nanoparticles,[1,2] silicon nanowire,[4,5] iron core-gold shell nanoparticles,[6] chitosan nanoparticles,[7] and gold nanorods[8] can kill tumor cells by apoptosis or necrosis.

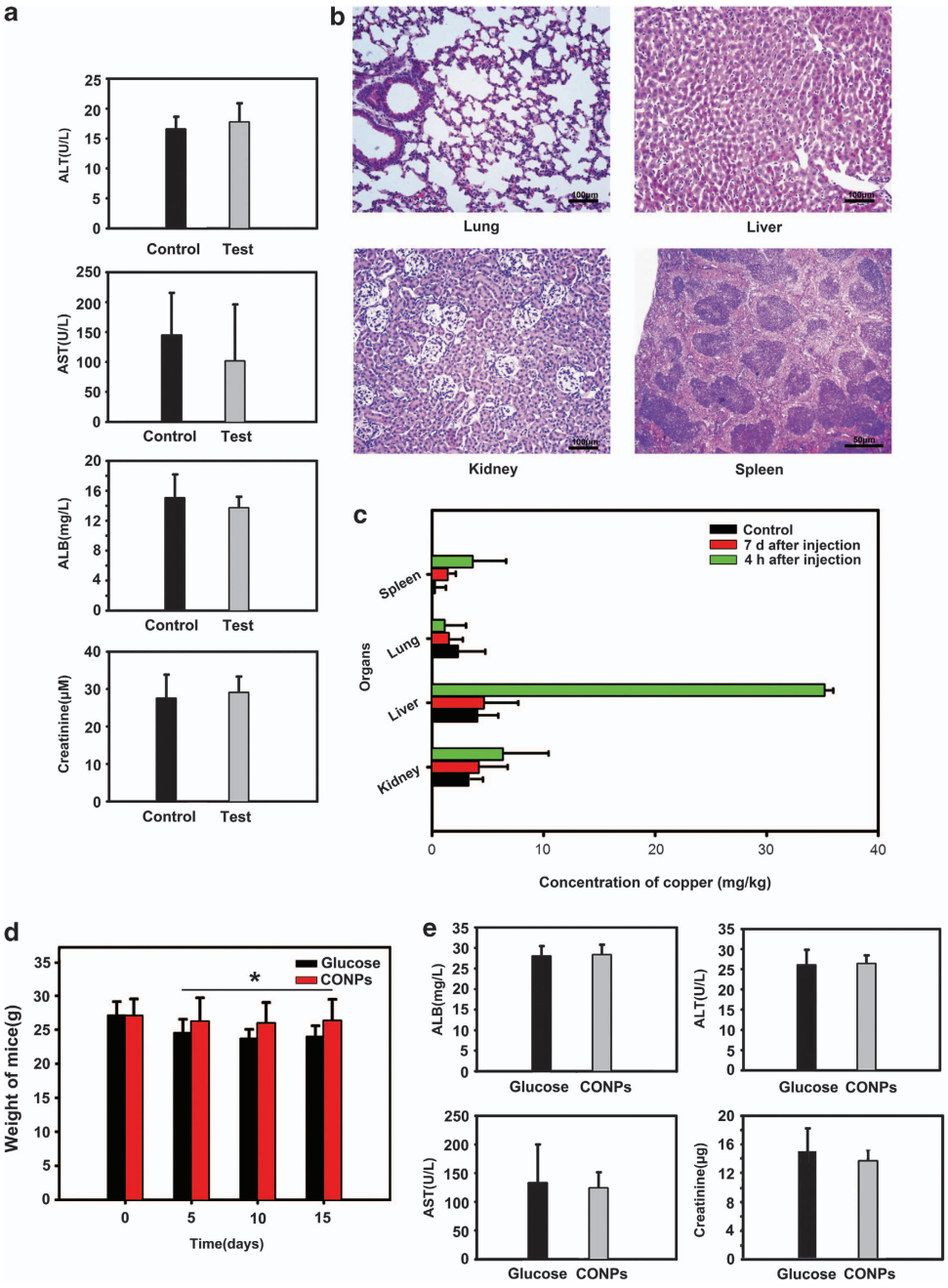

Figure 2 Assessment of toxicity and clearance of CONPs. (**a**) The serum alanine aminotransferase (ALT), aspartate aminotransferase (AST), albumin (ALB), and blood creatinine levels in the treatment group were the same as in the control group ($n = 4$). (**b**) HE-stained images of the major organs, showing that CONPs at a total dose of 6 mg/kg 1 day did not cause significant histological changes. (**c**) Mice were injected via the vena caudalis at a dose of 2 mg/kg. Four hours after the injection, the concentration of copper in the tested organs increased obviously. Seven days later, the concentration of copper in the tested organs had returned to normal, which suggested that the CONPs had been effectively cleared by the mice ($n = 4$). (**d**) Plot of weight changes in the mice bearing metastatic lung tumors. The weights of the CONP group were stable, whereas the weight of the mice in the glucose group decreased dramatically from day 5 to day 15 (*$P < 0.05$, Student's paired *t*-test), which indicated that the CONPs inhibited tumor growth with low systemic toxicity ($n = 6$). (**e**) The levels of serum ALT, AST, ALB, and blood creatinine in the mice with the metastatic lung tumors remained normal after treatment with CONPs and glucose for 15 days (all $P > 0.05$, Student's paired *t*-test, $n = 6$)

Previously, we described the anti-tumor activities of CONPs *in vitro.* In this research, we found that CONPs decreased the cell viability, induced apoptosis significantly, and inhibited the migration and invasion of B16-F10 cells *in vitro*. To further explore the anti-tumor capacity of CONPs *in vivo*, we used the particles to treat mouse subcutaneous melanoma and metastatic lung tumors, based on B16-F10 mouse melanoma cells, by intratumoral and systemic injections, respectively. The results exhibited that CONPs not only significantly delayed the growth of subcutaneous melanoma but also

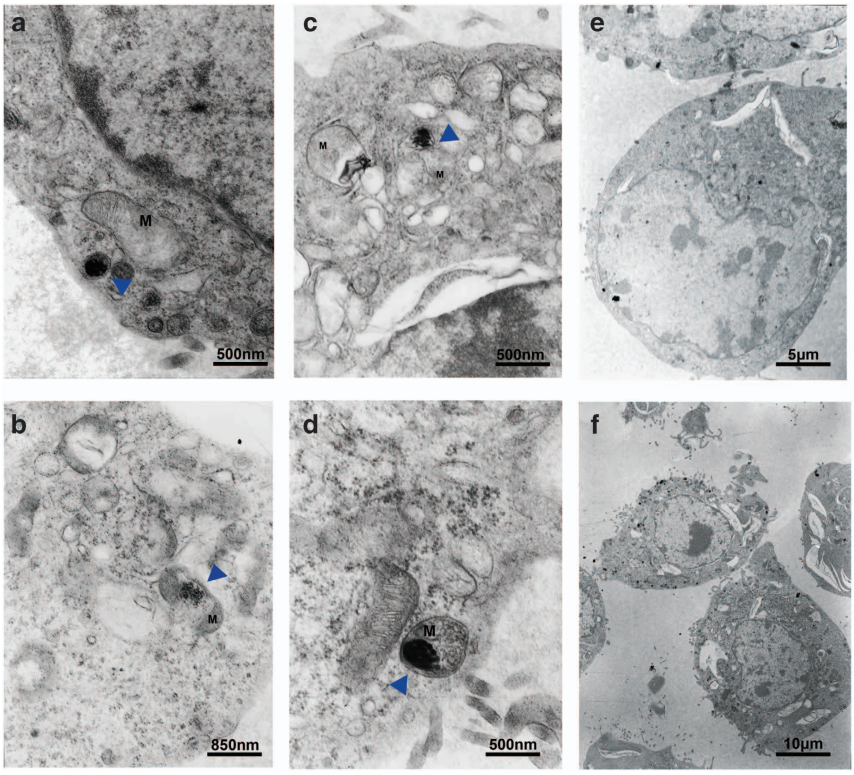

Figure 3 Determination of subcellular localization of CONPs by TEM. (**a**) CONPs entered the cells by endocytosis, were transported in a vesicle, and caused mitochondrion swelling. (**b**) CONPs broke the membrane of the mitochondrion and caused mitochondria swelling. (**c**) A vesicle containing CONPs touched the outer membrane of a mitochondrion. (**d**) CONPs entered a mitochondrion. (**e** and **f**) CONPs caused apoptosis of B16-F10 cells significantly. The cells showed obvious apoptotic phenotypes. (M, mitochondrion; CONPs in the cells were marked by the blue arrowheads)

increased the survival rate of tumor-bearing mice without damage to the organs of tumor-bearing mouse. These results are consistent with our previous *in vitro* results that CONPs selectively induce the apoptosis of tumor cells.

As we know, metastasis capacity of melanoma is one of the greatest challenges in melanoma therapy, because surgical interventions, radiation, and cytotoxic chemotherapies are all ineffective in repressing metastasis. In this research, we discovered that CONPs dramatically inhibited the metastasis of melanoma cells in the mice models with metastatic lung melanoma. To the best of our knowledge, this is the first study to report that CONPs inhibit the metastasis of tumor cells. We also did some research about the anti-metastasis mechanism of CONPs. We detected decrease of EMT-related gene expression, including *N-cadherin* (one of the marker genes of mesenchymal cell phenotype), *Twist1* and *Snail1* (both of them promote EMT progress of tumor cells),[24,25] which suggested that CONPs might decrease or inhibit metastasis capacity by influencing the EMT process of melanoma cells. More interestingly, our results exhibited that CONPs decreased the number of metastasis tumor nodules significantly while concentration of CONPs in the lung could not be checked out. We speculate that the inhibition effects of CONPs on cell proliferation may not make significant contribution to the decreasing of metastatic nodule in the CONP-treated mice because of the low concentration of CONPs in the lung. However, the method we used to treat metastatic melanoma with CONPs, systemic therapy, may tend to weaken the implantation capacity of circulating tumor cells in the lung.[26–29] Additionally, recent studies clarified that melanoma stem cells have an essential role in metastasis and recurrence of human melanoma,[30,31] which inspired us to explore whether CONPs inhibit the metastasis of tumor cells by killing the melanoma cancer stem cells in the following study.

The low toxicity is a principal characteristic of potential medicine. Some reports pointed out that certain metal nanoparticles and metal oxide nanoparticles can hardly be cleared from the animal organism, which is one of the reasons why the nanoparticles lead to organ damage of experimental animals. As a result, it is considered that the toxicity and clearance of inorganic nanoparticles constitute a bottleneck for their biomedical use.[32] For example, Au NPs disrupt zebrafish eye development,[33] Ag NPs cause chromosomal abrasives,[34] and TiO_2 NPs cause brain injury.[35] These suggest that inorganic nanomaterials with different chemical characteristics display their toxicity in different ways. In our research, we found that CONPs were cleared from the tested organs of the mice very quickly and the amount of copper was returned to normal level 7 days after one-time injection of CONPs, which may contribute to the little toxicity of CONPs. Meanwhile, the weights of the tumor-bearing mice in the CONP group were constant; in contrast, the weights of the glucose group decreased dramatically during the 15 days of systemic therapy in the metastatic lung tumor model. In addition, both the serum level of several factors and acute toxicity assay indicated that CONPs showed little hepatoxicity

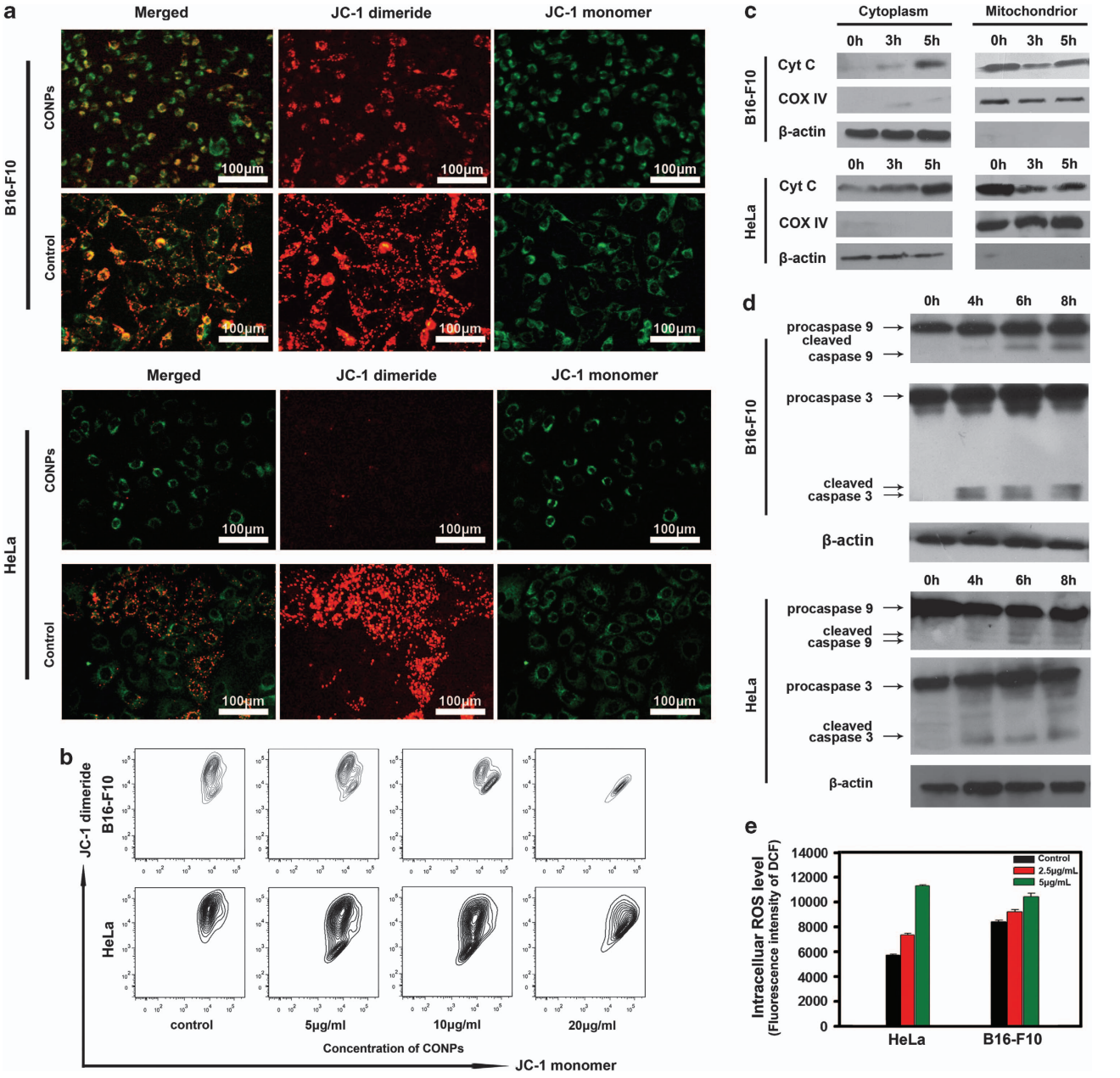

Figure 4 Mitochondrion-mediated apoptosis signaling pathway assay. (**a**) Fluorescence microscopic images of the B16-F10 and HeLa cells treated with CONPs (10 μg/ml) for 5 h. The red fluorescence intensity of the cells in the CONP group was weaker than in the control group. (**b**) Flow cytometry showed that the mitochondrial membrane potentials of the B16-F10 and HeLa cells decreased significantly after treatment with CONPs for 5 h. (**c**) Western blot assay of Cyt C release. The level of Cyt C increased in the cytoplasm and decreased in the mitochondria of the B16-F10 and HeLa cells treated with CONPs (5 μg/ml) for 3 or 5 h compared with the control (0 h). This finding indicated that the CONPs caused the release of Cyt C from the mitochondria. (**d**) Western blot assay of caspase-3 and caspase-9 activation. Caspase-3 and caspase-9 cleavage occurred in the B16-F10 cells and HeLa cells treated with CONPs. (**e**) ROS in the B16-F10 and HeLa cells were upregulated substantially and in a dose-dependent manner after being treated with CONPs for 5 h

or renal toxicity after 15-day systemic therapy with CONPs. Copper, at a low level, serves as co-factor for a variety of enzymes, such as cytochrome, and is essential to animals and higher plants. Further, cuprous is the low valence state of copper element, which may have even less toxicity than copper. CONPs when used in tumor therapy might be with less adverse effect than Ag NPs, Au NPs, and Ti NPs, or even some other types of anti-cancer drugs being used in the clinic.

It is reported that inorganic nanoparticles induced cell death by various pathways. Au NPs can inhibit MAPK and NF-κB signaling pathway and can cause DNA damage.[36,37] Ag NPs can inhibit the AKT, NF-κB signaling pathway, increase the activation of P53, P21, upregulate the Bax/Bcl-xl ratio, and cause DNA damage.[38,39] ZnO NPs can upregulate the expression of LC3, BECN1, which is associated with autophagy, and induce autophagic cell death.[40] Our research exhibited a different pathway that CONPs induce the

apoptosis of tumor cells. In our previous study,[19] TEM images showed that CONPs entered HeLa cells, targeted the mitochondrion, and broke the membranes of the mitochondria. Here we also observed that CONPs entered the mitochondria of B16-F10 cells. Mitochondria have a central role not only in energy metabolism but also in apoptosis of cells.[41] The current view is that the decrease of mitochondrial membrane potential is one of the earliest events in apoptosis,[42] which causes the release of Cyt C from the mitochondria and initiates the mitochondrion-mediated apoptosis signaling pathway. In the current study, we proved that the released Cyt C from mitochondrion activated caspase-9 and caspase-3, which are the two important downstream moleculars of the signaling pathway, and induced apoptosis of tumor cells. Furthermore, Z-VAD-FMK (carbobenzoxy-valyl-alanyl-aspartyl-[O-methyl]-fluoromethylketone) reversed the effects of CONPs on the tumor cells, which demonstrated that CONPs induced the apoptosis by activating apoptosis pathway mediated by caspases. We also discovered the rising of concentration of ROS in the B16-F10 cells and HeLa cells, which is a sign of mitochondrion disruption. These results suggested that CONPs could induce the apoptosis of tumor cells by mitochondrion-mediated apoptosis pathway. Some recent papers reported that carbon nanotube inhibits the synthesis of Cty C in cells, and gold nanotube with cetyltrimethyl ammonium bromide could target the mitochondria and induce apoptosis of cells.[43] The current study, for the first time, revealed that CONPs with no chemical modification target mitochondrion and initiate mitochondrion-mediated apoptosis pathway. Future studies may address the mechanism that CONPs target the mitochondria and that CONPs selectively induce the apoptosis of tumor cells.

In conclusion, CONPs inhibit the growth and metastasis of melanoma in tumor-bearing mice models and are rapidly cleared by mice with low toxicity. Additionally, CONPs target the mitochondria and induce apoptosis of cancer cells by initiating mitochondrion-mediated apoptosis signaling pathway (Figure 5). Thus, CONPs have ideal anti-tumor characteristics and are a good choice for us to develop and design a novel anti-tumor drug in melanoma therapy.

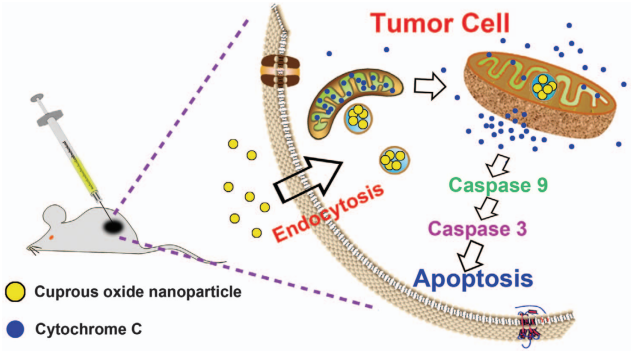

Figure 5 CONPs can significantly reduce the growth of melanoma *in vivo by* targeting the mitochondria and initiating the mitochondrion-mediated apoptosis signaling pathway

Materials and Methods

CONPs synthesis. CONPs were synthesized according to our previously reported protocol.[19]

***In vitro* cytotoxicity assay.** The HeLa cells and B16-F10 cells used in this research were grown in RPMI 1640 medium (Hyclone, Logan, UT, USA). This medium was supplemented with 2 mg/ml sodium bicarbonate, 4.5 mg/ml glucose, 100 μg/ml streptomycin sulfate, 40 μg/ml gentamicin, and 100 U/ml penicillin. The RPMI 1640 medium was also supplemented with 10% (vol/vol) heat-inactivated fetal calf serum. The cells were maintained in an environment of humidified air at 37 °C containing 5% CO_2, and both the cell lines were stored in our laboratory. The original source of the HeLa and B16-F10 cells was the Cell Bank of the Type Culture Collection (Chinese Academy of Sciences, Shanghai, China). To evaluate the cytotoxicity of the CONPs, cells in the log growth phase were seeded onto a 96-well culture plate at 1000 cells per well and incubated at 37 °C in a CO_2 incubator for 24 h until the cells adhered to the plate. Serial dilutions of CONPs were then added. After 24, 48, and 72 h, cell viability was measured using the MTT assay. In this assay, 200 μl of 5 mg/ml MTT solution (prepared in RPMI 1640 medium without serum) was added to the cells and incubated at 37 °C in a CO_2 incubator for 4 h. Dimethyl sulfoxide was then used to dissolve the formazan crystals, after which the absorbance was measured at 570 nm using an ELISA plate reader (Tiilitie, Finland).[43]

Apoptosis detection by Annexin V/PI staining. Cells in the log-phase were seeded onto a six-well culture plate at a density of 1×10^5 cells per well and incubated at 37 °C in a CO_2 incubator in the presence of CONPs. The cells were treated with 1.25, 2.5, 5, or 10 μg/ml CONPs. After 24 and 48 h, apoptosis and necrosis were analyzed with the Annexin V–fluorescein isothiocyanate apoptosis detection kit following the manufacturer's instructions. The samples were analyzed using a FACSCalibur flow cytometer (Becton Dickinson, San Jose, CA, USA).[19]

***In vitro* cell migration and invasion assays.** To explore the anti-migration effects of CONPs on the B16-F10 cells, 1×10^4 cells were seeded on a Matrigel (R&D Systems, Minneapolis, MN, USA) coated polycarbonate membrane insert (6.5 mm in diameter with 8.0-μm pores) in a 24-well culture transwell apparatus (Costar, Cambridge, MA, USA) and cultured in RPMI 1640 media with 0.5% fetal bovine serum. CONPs were added in the upper chamber at the final concentration of 0, 1.25, and 2.5 μg/ml. RPMI 1640 media with 10% fetal bovine serum was added to the lower chamber. After incubation for 16 h at 37 °C in a CO_2 incubator, the cells on the top surface of the insert were removed by wiping with a cotton swab. Cells that migrated to the bottom surface of the insert were fixed with paraformaldehyde, stained with feosin, and scored visually in five random fields using a light microscope. For the cell invasion assay, the procedure was similar to the cell migration assay, except that the transwell membranes were not coated with Matrigel (R&D Systems).[44]

Real-time RT-PCR of EMT-related genes. To verify the effects of CONPs on EMT, we measured the expression of EMT-related genes (*E-cadherin*, *N-cadherin*, *Snail1*, *Twist1*) in melanoma cells. B16-F10 cells were treated with CONPs for 48 h at the concentration of 1.25 and 2.5 μg/ml. Then, the real-time RT-PCR was carried out to explore the expression of EMT genes. Total RNA was extracted using TRIzol reagent (Invitrogen, Carlsbad, CA, USA) and purified using an RNeasy Mini column (Qiagen, Hilden, Germany) according to the manufacturers' protocols. Two microgram of purified total RNA was reverse transcribed to cDNA with the random primers and MultiScribe Reverse Transcriptase (Applied Biosystem, Foster City, CA, USA). The relative gene expression levels were measured by real-time RT-PCR using the gene-specific primers and iQ SYBRR Green Supermix (Bio-Rad, Philadelphia, PA, USA) and compared with the RPL13a RNA quantity for each cDNA sample as an endogenous control. Glyceraldehyde-3-phosphate dehydrogenase (*GAPDH*) was used as an endogenous RNA reference gene. Gene expression was normalized to the expression of *GAPDH*. Primers and product sizes for *E-cadherin (Cdh1)*, *N-cadherin (Cdh2)*, *Snail1*, and *Twist1* are summarized as follows:

Cdh1 (F) (5′-CAGGTCTCCTCATGGCTTTGC-3′), *Cdh1* (R) (5′-CTTCCGAAAAGAAGGCTGTCC-3′);

Cdh2 (F) (5′-TGACAATGGAATCCCGCCTA-3′), *Cdh2* (R) (5′-AAATCACCATTAAGCCGGTTG-3′);

Snail1 (F) (5′-AAGATGCACATCCGAAGC-3′), *Snail1* (R) (5′-ATCTCTTCACATCCGAGTGG-3′); and

Twist1 (F) (5′-CGGGTCATGGCTAACGTG-3′), *Twist1* (R) (5′-CAGCTTGCC ATCTTGGAGTC-3′).[26–28]

***In vivo* anti-tumor property assay of mice with subcutaneous melanoma.** B16-F10 cells were cultured in RPMI 1640 and suspended at 2×10^6 cells/ml in PBS directly before injection. For the subcutaneous tumor studies, male, 8–9-week-old C57BL/6 mice were sedated with tribromoethanol (Sigma, St Louis, MO, USA). The right hind leg was shaved before a subcutaneous injection of 100 μl cellular suspension. The tumors were monitored, and treatment began when the average tumor diameter reached 5–7 mm, typically 5–7 days after the injection. The mice in the CONP treatment group were injected intratumorally with CONPs at a dose of 16 mg/kg each day, whereas the control mice were injected with 5% glucose solution at the same volume as the CONPs. CONPs were dissolved in a 5% glucose solution using an ultrasonic mixer (Bilon, Shanghai, China). All the observers were blinded in the studies related to tumor area and survival rates. Six mice per group were euthanized at different time points, and the tumors were extracted and weighed.[45]

In the survival rate study, the new groups of mice with subcutaneous melanoma were injected as before and observed for 30 days. There were six mice per group, and the number of surviving mice was recorded each day.

To test for apoptosis or necrosis in a subcutaneous tumor of the CONP-treated and control mice on day 8, resected tumor tissue was fixed in 4% paraformaldehyde for at least 24 h and then embedded in paraffin. Tissue blocks were sectioned into 3-μm slices and mounted on glass slides. The TUNEL assay was then performed according to the manufacturer's instructions of *in situ* cell death detection kit (Roche, Mannheinm, Germany).

***In vivo* anti-tumor property assay of metastatic lung tumors.** Metastatic B16-F10 melanomas were established in male 8–9-week-old C57BL/6 mice by the intravenous (tail vein) administration of 100 μl B16-F10 cellular suspension, as previously described. Each group contained six mice. Treatment was initiated 1 day later and continued for 15 days, with a dose of CONPs (dissolved in 5% glucose solution) administered intravenously at 2 mg/kg each day via the vena orbitalis posterior. After killing, the lungs of the mice were perfused with 40 ml physiological saline. The lung metastases, the diameters of which were >0.1 mm, were counted using an anatomical lens.[45]

Assessment of acute toxicity and clearance of CONPs. Acute toxicity was assessed in healthy male C57BL/6 mice 7 days after an intravenous dose of CONPs or 5% glucose solution (control). CONPs were injected via the vena caudalis three times, achieving a whole dose of 6 mg/kg. After killing, the serum and major organs of the mice in the treatment and control groups were collected for further testing of hepatotoxicity and renal toxicity by the measurement of serum alanine aminotransferase, aspartate aminotransferase, albumin, and blood creatinine levels. The weights of the mice were also recorded each afternoon.

To explore the clearance of the CONPs, the C57BL/6 mice in the two treatment groups were injected with particles via the vena caudalis at a dose of 2 mg/kg, and the control mice were injected with 5% glucose solution at the same volume. The major organs of one treatment group were collected 4 h later. The other treatment group was maintained normally for 7 days, and then the major organs were also collected. All the organs were weighed and resolved in a perchloric acid/nitric acid admixture. After the organs were resolved, the mixtures were boiled until no white smoke volatilized, cooled, and adjusted to a volume of 1 ml. The concentrations of copper in samples were then tested using an atomic absorption spectrometer (Hitachi-Z5000, Tokyo, Japan).[46]

TEM. B16-F10 cells were grown in a large petri dish. When the cells had adhered to the dish, a solution of CONPs was added to a final concentration of 30 μg/ml. The cells were then incubated at 37 °C in a CO_2 incubator. After approximately 4–5 h, the cells were harvested, washed twice with PBS, and incubated in 4 °C formaldehyde overnight to fix the cells. The cells were dehydrated with increasing concentrations of ethanol (50, 60, 70, 80, 90, and 100%) for 15 min each, stained with 2% uranyl acetate in 70% ethanol overnight at room temperature, and embedded in Epon. The embedded samples were sectioned into 60-nm-thick slices using a sliding ultramicrotome, and the thin sections, supported by copper grids, were examined using a Hitachi TEM system (Hitachi-Z5000) operated at 100 kV.

Measurement of mitochondrial membrane potential. B16-F10 and HeLa cells were treated with CONPs (5, 10, or 20 μg/ml) for 5 h in six-well plates. The mitochondrial membrane potential was monitored using a fluorescent cationic dye known as JC-1 from the JC-1 mitochondrial membrane potential detection kit (Biotium, Hayward, CA, USA). In healthy cells, JC-1 enters the negatively charged mitochondria, where the dye aggregates and fluoresces red. In cells in which the mitochondrial membrane potential has collapsed, JC-1 exists as monomers throughout the cell. When dispersed in this manner, JC-1 fluoresces green. Consequently, mitochondrial depolarization is indicated by a decrease in the red–green fluorescence intensity ratio. Data acquisition was performed using a FACSCalibur flow cytometer (Becton Dickinson), and the data were analyzed using FlowJo software (Tree Star, Inc., Ashland, MA, USA). The cells treated with CONPs at a concentration of 10 μg/ml were also observed under a fluorescence microscope (Nikon, Tokyo, Japan).[46]

Western blotting analysis. Briefly, B16-F10 and HeLa cells were treated with CONPs at a concentration of 5 μg/ml. After treatment for 0, 3, or 5 h, the cells were pelleted by centrifugation and washed twice with ice-cold PBS. The resultant cell pellets were resuspended in 1 ml cytosol extraction buffer mix containing DTT and protease inhibitor and incubated for 15 min on ice. After homogenization, the unbroken cells and large debris were removed by centrifugation. The supernatants were saved as cytosolic extracts and stored at -80 °C, whereas the pellets were resuspended in 100-μl extraction buffer mix containing DTT and protease inhibitor and saved as mitochondrial fractions. The cytosolic and mitochondrial fractions isolated from the cells was loaded on a 12.5% SDS-PAGE gel, followed by western blotting with an anti-Cyt C antibody (CST, Danvers, MA, USA). The bound antibody was detected with peroxidase-conjugated anti-rabbit antibody followed by chemiluminescence (ECL System, Waltham, MA, USA) and exposed by autoradiography. The same blots were probed for COX IV (CST) and β-actin (CST), which are proteins in the cytoplasm and mitochondrial matrix.[47]

Caspase-3 and caspase-9 activity assays. The activity of caspase-3 and caspase-9 was determined using Caspase-3 and Caspase-9 Colorimetric Assay Kit from Abcam (Cambridge, MA, USA). Briefly, B16-F10 and HeLa cells were treated with CONPs at a concentration of 5 μg/ml. To evaluate the activity of caspase-3 and caspase-9, cell lysates were prepared after CONPs or control treatment for 0, 4, 6, or 8 h. The assays were performed in 96-well plates by incubating 20 μl cell lysate protein per sample in 70 μl reaction buffer (1% NP-40, 20 mM Tris-HCl (pH 7.5), 137 mM Nad, and 10% glycerol) containing 10 μl caspase-3 or caspase-9 substrate (2 mM). The lysates were then incubated at 37 °C for 4–12 h, after which the samples were assayed using an ELISA reader at an absorbance of 405 nm. Furthermore, we also tested the caspase-3 activation in the subcutaneous melanoma treated with CONPs in the '*In vivo* anti-tumor property assay of mice with subcutaneous melanoma' part, and the subcutaneous melanoma samples were stored at -80 °C.[48]

To test the caspase-3 and caspase-9 activities using another method, western blot was also carried out. Briefly, B16-F10 and HeLa cells were treated with CONPs at a concentration of 5 μg/ml. To evaluate the activity of caspase-3 and caspase-9, cell lysates were prepared after CONP treatment for 0, 4, 6, or 8 h. All cells, including no adherent cells in the supernatant, were washed twice in cold PBS and then lysed by gentle rotation in 500 ml of lysis buffer (150 mM NaCl, 10% glycerol, 1% Triton X-100, 2 mM EDTA, 1 mM PMSF, 40 mg/ml aprotinin, 20 mg/ml leupeptin) for 1 h on the ice. After the lysates were spun at 10 000 r.p.m. for 10 min, the supernatant was retained and loaded on a 12.5% SDS-PAGE gel followed by western blotting with an anti-Caspase-3 and anti-Caspase-9 antibody (CST). The same blots were probed for β-actin (CST), which is a protein in the cytoplasm.

Z-VAD-FMK blocking assay. Z-VAD-FMK is a cell-permeant pan caspase inhibitor that irreversibly binds to the catalytic site of caspase proteases and can inhibit induction of apoptosis. To explore whether the CONPs induce the apoptosis by the caspase-mediated pathway, the Z-VAD-FMK blocking assay was carried out. The HeLa cells and B16-F10 cells used in this research were grown as we did in the MTT assay. To evaluate Z-VAD-FMK effects, cells in the log growth phase were seeded onto a 96-well culture plate at 1000 cells per well and incubated at 37 °C in a CO_2 incubator for 24 h until the cells adhered to the plate. Before serial dilutions of CONPs were added, the Z-VAD-FMK was added in the medium at the final concentration of 20 μM.[49] After 24 h, and 48 h, cell viability was measured using the MTT assay as we did before.

Intracellular oxidative activity assay. Determination of the intracellular ROS levels was performed using a DCFDA-Cellular Reactive Oxygen Species

Detection Assay Kit from Abcam. After treatment with CONPs at a concentration of 2.5 or 5 μg/ml for 5 h, the cells were harvested, washed three times with PBS, and then treated with 10 μM dihydrodichlorofluorescein diacetate (DCF-DA) in serum-free RPMI 1640 medium at 37 °C for 30 min, followed by harvesting in serum-free medium. The cells were washed three times with serum-free medium, after which the DCF fluorescence was measured by a BD FACSCanto instrument (Becton Dickinson).[50]

Data and statistical analyses. Data are presented as means ± S.D. Student's paired *t*-tests and ANOVA were used to analyze differences in tumor masses, lung tumor metastases, toxicity, and so on. Log-rank test was used to analyze the difference in survival rate. Significance was established at $P < 0.05$.

Conflict of Interest

The authors declare no conflict of interest.

Acknowledgements. We thank Zhi-Fang Xie, Zhi-Ying He, Bing Yu, and Dao Xiang of the Department of Cell Biology for their helpful discussions and assistance with the procedures. This work was supported by the National Basic Research Program of China (Grant numbers 2010CB945600, 2011CB966200, and 2009CB941100), the National Natural Science Foundation of China (Grant numbers 30971462, 31171309, and 30600545), and the Basic Research Key Foundation of Shanghai (Grant number 13JC1401402).

Author contributions

YW performed the majority of the experiments and contributed to manuscript preparation. YPH and HYZ designed the whole article and contributed to the manuscript preparation. FY tested the samples using an atomic absorption spectrometer and western blot. HXZ and XYZ provided important technical assistance on the mice injection and tumor-bearing mice model. XHP made great contribution to the manuscript preparation. FC and JXL made great contribution on the TEM assay. WDL provided technical assistance on the HE staining. All authors read and commented on the paper.

1. Park J, Wrzesinski SH, Stern E, Look M, Criscione J, Ragheb R *et al.* Combination delivery of TGF-inhibitor and IL-2 by nanoscale liposomal polymeric gels enhances tumour immunotherapy. *Nat Mater* 2012; **11**: 895–905.
2. Yao L, Daniels J, Moshnikova A, Kuznetsov S, Ahmed A, Engelman DM *et al.* pHLIP peptide targets nanogold particles to tumors. *Proc Natl Acad Sci USA* 2013; **110**: 465–470.
3. Parka S, Sona YJ, Leong KW, Yoo HS. Therapeutic nanorods with metallic multi-segments:thermally inducible encapsulation of doxorubicin foranti-cancer therapy. *Nano Today* 2012; **7**: 76–84.
4. Su Y, Wei X, Peng F, Zhong Y, Lu Y, Su S *et al.* Gold nanoparticles-decorated silicon nanowires as highly efficient near-infrared hyperthermia agents for cancer cells destruction. *Nano Lett* 2012; **12**: 1845–1850.
5. Park G-S, Kwon H, Kwak DW, Park SY, Kim M, Lee J-H *et al.* Full surface embedding of gold clusters on silicon nanowires for efficient capture and photothermal therapy of circulating tumor cells. *Nano Lett* 2012; **12**: 1638–1642.
6. Wu YN, Chen DH, Shi XY, Lian CC, Wang TY, Yeh CS *et al.* Cancer-cell-specific cytotoxicity of non-oxidized iron elements in iron core-gold shell NPs. *Nanomedicine* 2011; **7**: 420–427.
7. Guan M, Zhou Y, Zhu QL, Liu Y, Bei YY, Zhang XN *et al.* N-trimethyl chitosan nanoparticle-encapsulated lactosyl-norcantharidin for liver cancer therapy with high targeting efficacy. *Nanomedicine* 2012; **8**: 1172–1181.
8. Wang Y, Black KC, Luehmann H, Li W, Zhang Y, Cai X *et al.* Comparison study of gold nanohexapods, nanorods, and nanocages for photothermal cancer treatment. *ACS Nano* 2013; **7**: 2068–2077.
9. Lee SK, Kim GS, Wu Y, Kim DJ, Lu Y, Kwak M *et al.* Nanowire substrate-based laser scanning cytometry for quantitation of circulating tumor cells. *Nano Lett* 2012; **12**: 2697–2704.
10. Dicheva BM, ten Hagen TLM, Li L, Schipper D, Seynhaeve ALB, van Rhoon GC *et al.* Cationic thermosensitive liposomes: a novel dual targeted heat-triggered drug delivery approach for endothelial and tumor cells. *Nano Lett* 2013; **13**: 2324–2331.
11. Kanapathipillai M, Mammoto A, Mammoto T, Kang JH, Jiang E, Ghosh K *et al.* Inhibition of mammary tumor growth using lysyl oxidase-targeting nanoparticles to modify extracellular matrix. *Nano Lett* 2012; **12**: 3213–3217.
12. Zhao G, Rodriguez BL. Molecular targeting of liposomal nanoparticles to tumor microenvironment. *Int J Nanomedicine* 2013; **8**: 61–71.
13. Chen Z, Wang ZY, Chen SJ. Acute promyelocytic leukemia: cellular and molecular basis of differentiation and apoptosis. *Pharmacol Ther* 1997; **76**: 141–149.
14. Roesch A, Fukunaga-Kalabis M, Schmidt EC, Zabierowski SE, Brafford PA, Vultur A *et al.* A temporarily distinct subpopulation of slow-cycling melanoma cells is required for continuous tumor growth. *Cell* 2010; **141**: 583–594.
15. Finger EC, Cheng CF, Williams TR, Rankin EB, Bedogni B, Tachiki L *et al.* CTGF is a therapeutic target for metastatic melanoma. *Oncogene* 2013. Available online on the website, http://www.nature.com/onc/journal/vaop/ncurrent/full/onc201347a.html.
16. Karreth FA, Tay Y, Perna D, Ala U, Tan SM, Rust AG *et al. In vivo* identification of tumor-suppressive PTEN ceRNAs in an oncogenic BRAF-induced mouse model of melanoma. *Cell* 2011; **147**: 382–395.
17. Sundstrøm T, Daphu I, Wendelbo I, Hodneland E, Lundervold A, Immervoll H *et al.* Automated tracking of nanoparticle-labeled melanoma cells improves the predictive power of a brain metastasis model. *Cancer Res* 2013; **73**: 2445–2456.
18. Fernandez-Cabezudo MJ, El-Kharrag R, Torab F, Bashir G, George JA, El-Taji H *et al.* Intravenous administration of manuka honey inhibits tumor growth and improves host survival when used in combination with chemotherapy in a melanoma mouse model. *PLoS One* 2013; **8**: e55993.
19. Wang Y, Zi XY, Su J, Zhang HX, Zhang XR, Zhu HY *et al.* Cuprous oxide nanoparticles selectively induce apoptosis of tumor cells. *Int J Nanomedicine* 2012; **7**: 2641–2652.
20. Dam DH, Lee JH, Sisco PN, Co DT, Zhang M, Wasielewski MR *et al.* Direct observation of nanoparticle-cancer cell nucleus interactions. *ACS Nano* 2012; **6**: 3318–3326.
21. Ma X, Zhang LH, Wang LR, Xue X, Sun JH, Wu Y *et al.* Single-walled carbon nanotubes alter cytochrome c electron transfer and modulate mitochondrial function. *ACS Nano* 2012; **6**: 10486–10496.
22. Huanga JG, Leshuk T, Gu FX. Emerging nanomaterials for targeting subcellular organelles. *Nano Today* 2011; **6**: 478–492.
23. Wang L, Liu Y, Li W, Jiang X, Ji Y, Wu X *et al.* Selective targeting of gold nanorods at the mitochondria of cancer cells: implications for cancer therapy. *Nano Lett* 2011; **11**: 772–780.
24. Méndez-Vidal C, Gámez-Del Estal Mdel M, Moreno-Mateos MA, Espina-Zambrano AG, Torres B, Pintor-Toro JA. PTTG2 silencing results in induction of epithelial-to-mesenchymal transition and apoptosis. *Cell Death Dis* 2013; **4**: e530.
25. Kushiro K, Núñez NP. Ob/ob serum promotes a mesenchymal cell phenotype in B16BL6 melanoma cells. *Clin Exp Metastasis* 2011; **28**: 877–886.
26. Onstenk W, Gratama JW, Foekens JA, Sleijfer S. Towards a personalized breast cancer treatment approach guided by circulating tumor cell (CTC) characteristics. *Cancer Treat Rev* 2013; **39**: 691–700.
27. Ozkumur E, Shah AM, Ciciliano JC, Emmink BL, Miyamoto DT, Brachtel E. Inertial focusing for tumor antigen-dependent and -independent sorting of rare circulating tumor cells. *Sci Transl Med* 2013; **5**: 179ra47.
28. Tirino V, Camerlingo R, Bifulco K, Irollo E, Montella R, Paino F *et al.* TGF-β1 exposure induces epithelial to mesenchymal transition both in CSCs and non-CSCs of the A549 cellline, leading to an increase of migration ability in the CD133+ A549 cell fraction. *Cell Death Dis* 2013; **4**: e620.
29. Lane N, Martin W. The energetics of genome complexity. *Nature* 2010; **467**: 929–934.
30. Boiko AD, Razorenova OV, van de Rijn M, Swetter SM, Johnson DL, Ly DP *et al.* Human melanoma-initiating cells express neural crest nerve growth factor receptor CD271. *Nature* 2010; **466**: 133–137.
31. Civenni G, Walter A, Kobert N, Mihic-Probst D, Zipser M, Belloni B *et al.* Human CD271-positive melanoma stem cells associated with metastasis establish tumor heterogeneity and long-term growth. *Cancer Res* 2011; **71**: 3098–3109.
32. Soenen SJ, Rivera-Gil P, Montenegro J-M, Parak WJ, De Smedt SC, Braeckmans K. Cellular toxicity of inorganic nanoparticles: Common aspects and guidelines for improved nanotoxicity evaluation. *Nano Today* 2011; **6**: 446–465.
33. Kim KT, Zaikova T, Hutchison JE, Tanguay RL. Gold nanoparticles disrupt zebrafish eye development and pigmentation. *Toxicol Sci* 2013; **133**: 275–288.
34. Ghosh M, J M, Sinha S, Chakraborty A, Mallick SK, Bandyopadhyay M *et al. In vitro* and *in vivo* genotoxicity of silver nanoparticles. *Mutat Res* 2012; **749**: 60–69.
35. Ze Y, Zheng L, Zhao X, Gui S, Sang X, Su J *et al.* Molecular mechanism of titanium dioxide nanoparticles-induced oxidative injury in the brain of mice. *Chemosphere* 2013; **92**: 1183–1189.
36. Arvizo RR, Saha S, Wang E, Robertson JD, Bhattacharya R, Mukherjee P. Inhibition of tumor growth and metastasis by a self-therapeutic nanoparticle. *Proc Natl Acad Sci USA*. 2013; **110**: 6700–6705.
37. Sharma M, Salisbury RL, Maurer EI, Hussain SM, Sulentic CE. Gold nanoparticles induce transcriptional activity of NF-κB in a B-lymphocyte cell line. *Nanoscale* 2013; **5**: 3747–3756.
38. Satapathy SR, Mohapatra P, Preet R, Das D, Sarkar B, Choudhuri T *et al.* Silver-based nanoparticles induce apoptosis in human colon cancer cells mediated through p53. *Nanomedicine (Lond)* 2013; **8**: 1307–1322.
39. Jeyaraj M, Rajesh M, Arun R, MubarakAli D, Sathishkumar G, Sivanandhan G *et al.* An investigation on the cytotoxicity and caspase-mediated apoptotic effect of biologically synthesized silver nanoparticles using Podophyllum hexandrum on human cervical carcinoma cells. *Colloids Surfaces B Biointerfaces* 2013; **102**: 708–717.
40. Yu KN, Yoon TJ, Minai-Tehrani A, Kim JE, Park SJ, Jeong MS *et al.* Zinc oxide nanoparticle induced autophagic cell death and mitochondrial damage via reactive oxygen species generation. *Toxicol in Vitro* 2013; **27**: 1187–1195.

41. Youle RJ, van der Bliek AM. Mitochondrial fission, fusion, and stress. *Science* 2012; **337**: 1062–1065.
42. Lin MT, Beal MF. Mitochondrial dysfunction and oxidative stress in neurodegenerative diseases. *Nature* 2006; **443**: 787–795.
43. Julien DC, Richardson CC, Beaux MF 2nd, McIlroy DN, Hill RA. *In vitro* proliferating cell models to study cytotoxicity of silica nanowires. *Nanomedicine* 2010; **6**: 84–92.
44. Zhang LJ, Chen L, Lu Y, Wu JM, Xu B, Sun ZG *et al.* Danshensu has anti-tumor activity in B16F10 melanoma by inhibiting angiogenesis and tumor cell invasion. *Eur J Pharmacol* 2010; **643**: 195–201.
45. Narver HL. Care and monitoring of a mouse model of melanoma. *Lab Anim (NY)* 2013; **42**: 92–98.
46. Chinnam P, Mohsin M, Shafee LM. Evaluation of acute toxicity of pioglitazone in mice. *Toxicol Int* 2012; **19**: 250–254.
47. Rathore S, Jain S, Sinha D, Gupta M, Asad M, Srivastava A *et al.* Disruption of a mitochondrial protease machinery in Plasmodium falciparum is an intrinsic signal for parasite cell death. *Cell Death Dis* 2011; **2**: e231.
48. Aprigliano I, Dudas J, Ramadori G, Saile B. Atorvastatin induces apoptosis by a caspase-9-dependent pathway: an *in vitro* study on activated rat hepatic stellate cells. *Liver Int* 2008; **28**: 546–557.
49. Zhang J, Yan H, Wu YP, Li C, Zhang GY. Activation of GluR6 containing kainate receptors induces ubiquitin-dependent Bcl-2 degradation viadenitrosylation in the rat hippocampus after kainate treatment. *J Biol Chem* 2011; **286**: 7669–7680.
50. Diaz B, Shani G, Pass I, Anderson D, Quintavalle M, Courtneidge SA. Tks5-dependent, Nox-mediated generation of reactive oxygen species is necessary for invadopodia formation. *Sci Signal* 2009; **2**: ra53.

Supplementary Information accompanies this paper on Cell Death and Disease website (http://www.nature.com/cddis)